Numerical Studies on Turbulent Separated Flows in High-Velocity Transient Motors

V.R. Sanal Kumar,[1] H.D. Kim,[2] B.N. Raghunandan,[3] and T. Setoguchi[4]

[1,2]School of Mechanical Engineering, Andong National University
Andong, Kyeongbuk 760-749, KOREA

[3]Department of Aerospace Engineering, Indian Institute of Science
Bangalore-12, Karnataka, INDIA

[4]School of Mechanical Engineering, Saga University
Honjo-machi, Saga 840-8502, JAPAN

Abstract

Numerical studies have been carried out to examine the starting transient flow features in high-performance solid rocket motors with non-uniform port geometry with the aid of a standard k-omega turbulence model. The parametric studies have been carried out to examine the geometry-dependent driving forces, which control the transient flow features of solid rockets with non-uniform ports. We concluded that the narrow port and long flow development ahead of the steep divergence are shown to favor flow separation, which might lead to high peak pressure, pressure-rise rate and thrust oscillations during the starting transient period of operation of high-velocity transient motors with divergent ports.

Introduction many modern high-performance solid rockets have grains with sudden expansion/divergence of port combined with high volumetric loading density, high throat to port area ratio ($A_t/A_p > 0.56$) and large length-to-diameter ratio ($L/D \geq 10$). Qualitatively these motors are referred as high-velocity transient (HVT) motors. Flow separation and recirculation caused by sudden changes in port geometry plays an important role in the design of these motors. The basic idea behind a solid rocket motor (SRM) is simple but its design is a complex technological problem requiring expertise in diverse sub disciplines to address all of the physics involved. The design optimization of high-performance rockets is more complex when the mission demands dual thrust. Dual-thrust motors with single chamber necessarily have non-uniform port geometry. Although, a great deal of research has been done in the area of solid rockets for more than six decades, the accurate prediction of the starting transient/ ignition transient of high-performance solid rockets with non-uniform ports has remained an intangible problem [1-3]. The starting transient is usually defined as the time interval between the application of the ignition signal and the instant at which the rocket motor attains its equilibrium or the designed operating conditions. The two primary concerns during the starting transient are the overall time of the transient and the extent of the peak pressure. The overall time, that is, the delay in the development of full thrust must be kept within some limit and must be reproducible. This research topic, although interesting in its own right, has been motivated by several practical problems.

The motivation for the present study emanates from the desire to explain the phenomena or mechanism(s) responsible for the high pressure, pressure-rise rate, instabilities and pressure oscillations

---
[1]Scientist/Engineer, Propulsion Group, Vikram Sarabhai Space Centre, India, Email: rsanal@hotmail.com (Currently at the Andong National University).
[2]Professor and Head
[3]Professor and Chairman
[4]Professor

often observed during the static tests and the actual flights of certain class of SRMs with non-uniform ports [3-6]. In this study attention is focused on idealized grain geometry with divergent port; deduced from the US Space shuttle's redesigned SRM, Ariane 5 SRM and Dual-thrust motor configurations. For technological reasons, large solid propellant boosters, such as US Space Shuttle and Titan SRMs or European Ariane 5 P230 are made from segmented propellant grains from three to seven segments with non-uniform ports according to the motor versions. Earlier works at the USA show that such grain segmentation conducted to low amplitude, but sustained pressure and thrust oscillations, on the first longitudinal acoustic mode frequencies [7-9]. Although such oscillations do not jeopardize the mission, they induce some penalties to the overall performance. Detailed studies on instabilities and pressure oscillations in solid rocket motors have been carried out by Yves Fabignon et al [7] at ONERA (2003). But none of these studies able to explain the cause(s) of the unexpected pressure peak, pressure-rise rate and thrust oscillations often observed in certain class of dual-thrust motors (DTMs) during the starting transient period of operation. Figure 1 shows a typical DTM configuration with narrow cylindrical port at the head-end followed by divergence region and star port at the nozzle-end. In such configurations, it is very likely that the flow separation would take place at transition locations.
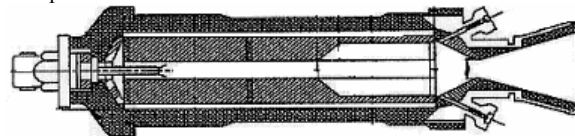
Figure 1. Typical dual-thrust motor.

In all the previous studies the features of turbulent separated flows are not examined in any motor with dual-thrust configuration [10]. With the advent of computational fluid dynamics (CFD) and available computer power, several numerical studies have been reported on the overall starting transient of SRMs in the recent past. Even though these studies have been helpful in interpreting many fundamental processes on starting transient, the understanding of pressure peak and pressure oscillations often observed in HVT motors has been elusive. In an attempt to resolve some of these problems and in the light of new findings [10, 11], a substantial revision of the existing idea is required. One such problem of urgency is to examine the starting transient flow features, without invoking the mass addition and combustion, of high-performance solid rockets with non-uniform ports. In this paper, using a two dimensional turbulence model, a diagnostic investigation is carried out to examine the geometry-dependent driving forces on the starting transient flow features of dummy (unignited) SRMs with dual thrust configuration. Note that it is often the practice in ignition studies to use dummy grains to obtain the physical insight into the starting transient flow features of SRMs *a priori*.

Numerical Method of Solution

The numerical simulations have been carried out with the help of a standard k-omega model. This turbulence model is an empirical model based on model transport equations for the turbulence kinetic energy (k) and the specific dissipation rate (ω). This code solves standard k-omega turbulence equations with shear flow corrections using the coupled second order implicit unsteady formulation. The turbulence kinetic energy, k, and the specific dissipation rate, ω, are obtained from the following two transport equations:

$$\frac{\partial}{\partial t}(\rho k) + \frac{\partial}{\partial x_i}(\rho k u_i) = \frac{\partial}{\partial x_j}\left(\Gamma_k \frac{\partial k}{\partial x_j}\right) + G_k - Y_k + S_k \tag{1}$$

$$\frac{\partial}{\partial t}(\rho \omega) + \frac{\partial}{\partial x_i}(\rho \omega u_i) = \frac{\partial}{\partial x_j}\left(\Gamma_\omega \frac{\partial \omega}{\partial x_j}\right) + G_\omega - Y_\omega + S_\omega \tag{2}$$

In the equations, G_k represents the generation of turbulent kinetic energy due to mean velocity gradient. G_ω represents the generation of ω. Γ_k and Γ_ω represent the effective diffusivity of k and ω, respectively. Y_k and Y_ω represent the dissipation of k and ω due to turbulence. S_k and S_ω are user-defined source terms.

This model uses a control-volume based technique to convert the governing equations to algebraic equations, which can be solved numerically. The viscosity is determined from the Sutherland formula. An algebraic grid-generation technique is employed to discretize the computational domain. The present code has been validated and selected for capturing the fine flow features often observed in SRMs with non-uniform port. A typical grid system in the computational region is selected after the detailed grid refinement exercises. The grids are clustered near the solid walls using suitable stretching functions. In all the cases length of the first grid from the solid surfaces is taken as 0.1 mm. The motors geometric variables and material properties are known *a priori*. Initial wall temperature, inlet total pressure and temperature are specified. At the solid walls no-slip boundary condition is imposed. At the nozzle exit a pressure profile is imposed. The Courant-Friedrichs-Lewy number is initially chosen as 3.0 in all of the computations. Ideal gas is selected as the working fluid. The transient mass additions due to propellant burning are deliberately ignored in this model to examine the turbulent separated flow features discretely in solid rockets with non-uniform ports.

The numerical results corresponding to the experimental configuration and propellant properties reproduce many qualitative features such as secondary ignition and backward flame spread. These results are succinctly reported in the previous connected papers [12-16]. In this study consideration is given to examine the geometrical influence on turbulent separated flows in SRMs without any mass addition. Results of interests such as reattachment length, size of the recirculation bubble and the axial velocity variations are reported to illustrate the influence of transition region on the flow characteristics of turbulent mixed convection downstream of a solid rocket motor with divergent port. Such detailed results are needed for an integrated design and optimization of the high-performance solid rockets port geometry and its allied igniters with confidence.

Results and Discussion

In the present numerical simulation two different physical models with different port geometries are examined. In the first phase low-velocity transient (LVT) motors ($A_t/A_p \leq 0.56$, $L/D \leq 10$) and in the second phase HVT motors are considered. The grid system (baseline case) in the computational region for LVT motor is shown in figure 2. Baseline values are selected based on the geometric configuration of a typical LVT motor ($L/D = 4$,
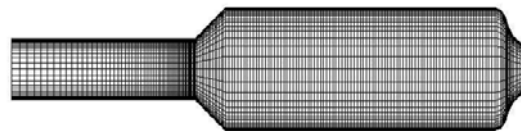
Figure 2. Grid system (180 x 30) in the computational region.

$X_s/d = 3$, $d_t/D = 0.375$). Initial total pressure and temperature are given as the input to the code and a pressure profile is imposed at the exit. Except the geometric variable all other parameters are kept constant in the parametric studies.

Figure 3 shows the comparison of the axial velocity variation at a particular time interval for five different test cases. In the first three cases divergent location (Xs) is varied, in the forth case inlet diameter is increased by 50% and in the fifth case divergence angle, α is increased from 45 $^\circ$ to 64 $^\circ$. All the results reported are anticipated and giving corroborative evidences of the previous experimental and theoretical findings [10-16].
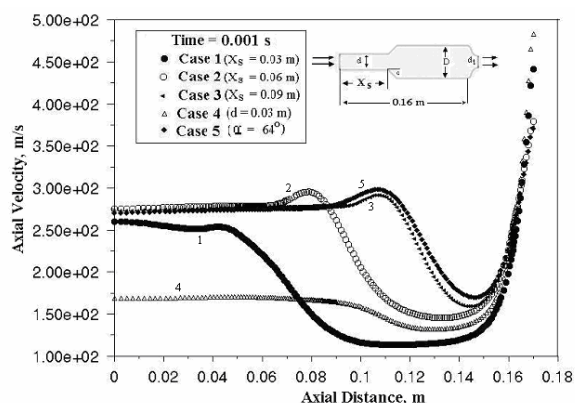
Figure 3. Demonstrating the influence of port geometry on the velocity variation along the axis (configuration is shown in inset).

It can be seen from figure 3 that, in three different cases (Case 2, 3 & 5), the axial velocity is relatively high at the divergence location. This can be explained with the help of boundary layer theory. Note that owing to the viscous friction, boundary layer will be formed on the walls (before the transition region) and their thickness will increase in the down stream direction to the divergence location. Since the volume of flow must be the same for every section, the decrease in rate of flow near the walls which is due to friction must be compensated by a corresponding increase near the axis. Thus the boundary layer growth occurs under the influence of an accelerated external flow. As a result, at larger distances from the inlet section velocity will be relatively high at the divergence location. This will cause flow separation far downstream of the divergence region. In the forth case reported herein shown relatively low velocity at the axis due to high port area compared to the other four cases reported. Traditionally many solid rocket motor designers occasionally increases the port area of a solid rocket motor for reducing the unexpected pressures peak observed during the starting transient period. Note that such an increase in port area will negate the high performance nature of the rocket motor. Figure 4 depicts the velocity vectors at two different time intervals showing the formation of recirculation bubble and flow reattachment for a typical case. This figure gives a clear description about the flow development pattern at the expansion region during the starting transient period of operation of a typical solid rocket motor with divergent port. The recirculation bubble and the reattachment point are visible at the divergent region at time, t=0.006s. When time advances this region gradually expands and shifts towards the downstream and finally vanishes. Reverse flow can be

recognized up to t = 0.001 s. This phenomenon is not observed in the forth case due to high inlet port area and low axial velocity.
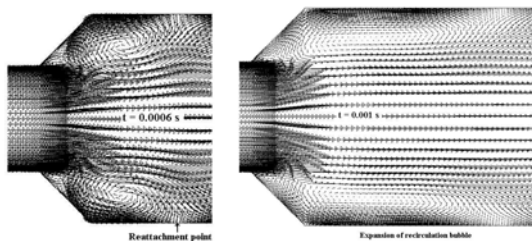
Figure 4. Sequence of pictures showing the formation of recirculation bubble and its expansion at two different intervals of time in an SRM with divergent port (Enlarged view).

In the first case flow recirculation tendency, leading for reattachment and secondary ignition, was found very less because location of the transition region was near to the head-end at the cost of the propellant loading density. When the transition location was fixed at far downstream of the SRM, the tendency of flow separation was found very high. This will lead to the formation of recirculation bubble and flow reattachment. Note that the flow reattachment will favour secondary ignition and that will cause the flow unsteadiness leading for an unacceptable high-pressure rise rate during the staring transient period of operation of solid rockets. Hence the prudent selection of the transition location within the given envelop, without diluting the high-performance nature of solid rocket motor, is critical for a designer. This task will be more complex in the case of HVT motor, which is discussed in the subsequent session.

In the second phase attention is focused on HVT motors with sudden enlargement of port, as has been observed in the case of Space Shuttle's Redesigned SRM. In the parametric study three different transition locations (X_s) are considered. Figure 5 shows the grid system in the computational region of the baseline case.

Figure 5. Grid system in the computational region of an HVT motor.

An algebraic grid-generation technique is employed to discretize the computational domain. The total element in each case is fixed as 1328. The grids are clustered using suitable stretching functions for capturing the fine flow features during the transient period. Note that the inappropriate stretching of grids will lead to the inaccurate prediction of the reattachment point. An error in pinpointing the reattachment point will lead to the significant errors in the actual prediction of the location of secondary ignition, which will warrant the inaccurate performance prediction of HVT motors. The geometrical parameters are selected based on typical HVT motors. In all the cases, considered in this study, the length-to-diameter ratio and the throat-to-port area ratio are retained as constant values similar to a conventional HVT motor. The igniter jet flow and the material properties are retained as constant for examining the influence of location of the transition region on identical conditions. The ignition is not invoked in this analysis. At the solid walls no-slip boundary condition is imposed. Initial total pressure and temperature are prescribed at the inlet and a pressure profile is imposed at the nozzle exit. In the first numerical drill, for all the cases, the initial igniter total pressure is taken as 2.25 kgf/cm^2, and temperature as 700 K. The turbulent intensity is assumed as 10% at the inlet and the exit. At the given inlet hydraulic diameter, using the standard k-ω model, the initial inlet turbulent kinetic energy is evaluated as 306.93 m^2/s^2 and the corresponding specific dissipation rate is obtained as 62569.78 s^{-1}. The initial Courant-Friedrichs-Lewy number is chosen as 5 in all the cases.

Figure 6 is demonstrating the difference in velocity magnitude along the axis of an HVT motor with three different divergent locations at two different time intervals but with same initial and boundary conditions. In all the cases the velocity magnitude is found maximum at the transition location.
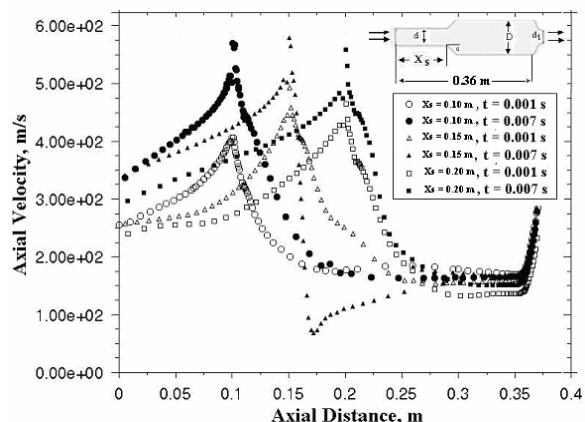
Figure 6. Demonstrating the difference in velocity magnitude along the axis of an HVT motor with three different divergent locations at two different time intervals but with same initial and boundary conditions.

As explained in the previous cases, in general, at larger distances from the inlet section (X_s) velocity will be high at the step location due to the boundary layer effect. But figure 6 shows that the peak value of the axial velocity is relatively lower in the Case 3 ($X_s = 0.20$ m) than the Case 2 ($X_s = 0.15$ m). This will not contradict the argument reported earlier based on boundary layer effect because this difference is due to the altered variation of the entire flow field due to the nozzle end effect coupled with the geometry dependent driving forces and the corresponding compressibility effect. Through these diagnostic investigations, we observed that there is a limiting case of the location for transition for developing maximum axial velocity in any HVT motor due to its port geometry. In all the HVT motor cases, as anticipated, at the upstream the flow acceleration is found very high compared to the LVT motor cases reported earlier.
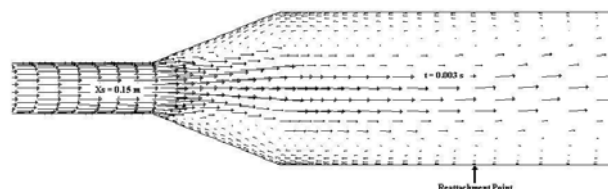
Figure 7. Velocity distribution showing the formation of the recirculation bubble and the reattachment point at the divergent region of the HVT motor of Case 2 ($X_s = 0.15$ s) at time, t = 0.003 s (Enlarged view).

The separated flow characteristics such as size of the separation bubble, flow redevelopment and heat transfer in the recirculation region are known to depend on Reynolds number upstream of the divergent region and its height. In the HVT motor cases considered here the reattachment point is found to lie around 1.5 - 3 times of the divergent height, as estimated, which is relatively higher than the LVT cases considered in this study. Figure 7 depicts the velocity vectors at time, t = 0.003 s showing the formation of recirculation bubble and flow reattachment for the case $X_s = 0.15$ m. Reverse flow can also be recognized in this figure. We can easily infer from this figure that the implication of the secondary ignition will be more severe in the case of HVT motors because the location of the secondary ignition will be closer to the reattachment point, which is observed far downstream than LVT motor cases. From these results one can assert that the flow instability, pressure-rise rate and the ignition pressure peak will be more prominent in HVT motors than LVT

motors. We also observed that in all the cases, due to the flow instability, the near wall temperature was found non-uniform along the curved surface and as a result the heat flux values will be discontinuous. This will warrant the discontinuous ignition leading for multiple flame fronts in HVT motors with divergent port. The velocity, density and temperature fluctuations are not independent, being related, also through pressure fluctuations, by the mass balance equation, the energy balance equation, and the constitutive equation of the fluid. So suppression and control of one parameter will be a meaningful objective for rocket motor design optimization. We also discerned that under certain conditions, the flow gets accelerated to a higher Mach number (M>1) near the transition region of an HVT motor with divergent port but without any geometrical-throat! A shock wave cannot exist unless the Mach number is supersonic; therefore the flow must have accelerated through a throat which is sonic. As argued above, owing to the viscous friction, boundary layer will be formed on the walls (before the transition region) and their thickness will increase in the down stream direction to the divergent location leading to the formation of a momentarily *fluid-throat* at the transition location. This might lead to the formation of shock waves in certain class of HVT motors with divergent port. Note that the downstream of the shock the flow has an adverse pressure gradient, usually leading to wall boundary-layer separation and reattachment.

From these studies one can deduce that the thrust/pressure oscillations, pressure-rise rate and unexpected peak pressure often observed in solid rockets with non-uniform ports are presumably contributed due the joint effects of the geometry dependent driving forces and the chamber gas dynamic forces. The present study is expected to aid the designer for conceiving the physical insight into problems associated with the prediction and the reduction of the peak pressure, the pressurization rate and thrust oscillations during the starting transient period of operation of solid rockets with non-uniform ports.

Concluding Remarks
It is indeed accepted that no single turbulence model is universally accepted as being superior for all class of problems. However, the experience gained through our studies prompted to choose k-omega model for the diagnostic investigation of the oscillatory behavior of thrust transient of solid rockets with non-uniform ports. Through these diagnostic investigations, we observed that there is a limiting case for transition location for forming peak velocity in any HVT motor due to the nozzle end effect coupled with the port geometry and the chamber gas dynamics effects. The shock waves, the boundary layer thickness and the turbulence are rather familiar notion: yet it is not easy to define in such a way as to cover the detailed flow characteristics comprehended in HVT motors. The shock waves in HVT motor will alter the turbulence level and this new turbulence level will alter the location of reattachment and secondary ignition. The shock wave formed presumably due to the *fluid-throat* effect is an area that needs to be contemplated in detail. We concluded that the narrow port and long flow development ahead of the steep divergence are shown to favour flow separation, which might lead to high pressure-rise rate and ignition over pressure during the starting transient of SRMs with non-uniform ports. The zone of the secondary ignition for many laboratory tests and the location of the reattachment point for SRMs with divergent port in the present numerical studies are found around 0.8-3.0 times of the step height. Therefore, one can conclude that the secondary ignition occurs inside the initial recirculation bubble. The preheating of the propellant in this zone before the arrival of the flame at the transition region therefore appears important, which however not invoked in this analysis. The present study leads to say that a prudent selection of the port geometry is one of the challenging tasks for any HVT motor designer for getting reliability, repeatability and payload capability of any launch vehicle with credence.

References
[1] Peretz, A., Kuo, K.K., Caveny, L.H., & Summerfield, M., Starting transient of solid propellant rocket motors with high internal gas velocities, *AIAA. Journal*, Vol. 11, No. 12, 1973, 1719-1729.
[2] Kumar, M. and Kuo, K. K, 1983, Flame spreading and overall ignition transient, *Prog. Astronaut. & Aeronaut*, 90, 1983, 305-60.
[3] Salita, M., Modern ignition transient modelling (Part 1): Introduction and Physical Models, *AIAA Paper*, No. AIAA 2001-3443.
[4] Raghunandan, B.N., *Diagnostic investigation of ignition problems in high-performance rocket motors*, Final Technical Report, AE Department, IISc, Bangalore, India, Report No. ISTC/AE/BNR/043, 1995.
[5] Sanal Kumar, V. R., and Raghunandan, B. N., A ballistic explanation of ignition peak of low velocity transient motors, *Proceedings of the 2nd IHEM Conference and Exhibit*, IIT Chennai, India, 8-10 Dec., 1998, 371-375.
[6] Luke, G. D., Eager. M. A., and Dwyer, H. A., Ignition transient model for large aspect ratio solid rocket motors, *AIAA paper*, No. AIAA 96-3273.
[7] Fabignon, Y., Dupays, J., Avalon. G., Vuillot, F., Lupoglazoff, N., Casalis, G and Prevost, M, Instabilities and pressure oscillations in solid rocket motors, *Aerospace Science and Technology*, 7, 2003, 191-200.
[8] Brown, R.S., Dunlup, R., Young, S.W., and Waugh, R.C., Vortex shedding as a source of acoustic energy in segmented solid rockets, *Journal of Spacecraft and Rockets* 18(4), 1981, 312-319.
[9] Manson, D.R., Folkman, S.K., Behring, M.A, Thrust oscillations of the space shuttle solid rocket booster motor during static tests, *AIAA paper* . No. AIAA 79-1138.
[10] Raghunandan, B. N., Sanal Kumar, V. R., Unnikrishnan, C and Sanjeev, C., 2001, Flame spread with sudden expansions of ports of solid propellant rockets, *Journal of Propulsion and Power*, Vol. 17, No. 1, 2001, 73-78.
[11] Sanal Kumar, V.R., Thermoviscoelastic characterization of a composite solid propellant using tubular test, *Journal of Propulsion and Power*, Vol.19, No.3, 2003, 397-404.
[12] Raghunandan,B.N., Madhavan, N.S., Sanjeev, C and Sanal Kumar, V. R., Studies on flame spread with sudden expansions of ports under elevated pressure, *Defence Science Journal*, 46 (5), 1996, 417-423.
[13] Sanal Kumar, V. R., and Unnikrishnan, C., Raghunandan, B.N., 2000, Studies on ignition transients of solid rocket motors with non-uniform ports, *AIAA Paper*, No.2000-3701.
[14] Unnikrishnan, C., Sanal Kumar, V. R., and Raghunandan, B.N., Internal flow simulation of solid rockets using an unsteady Navier Stokes solver, *AIAA Paper*, No.2001-3450.
[15] Sanal Kumar, V. R., and Unnikrishnan, C., Raghunandan, B.N., Effect of flame spread mechanism on starting transients of solid rocket motors, *AIAA Paper*, No. 2001-3854.
[16] Sanal Kumar, V. R., Unnikrishnan, C., Kim, H.D., Raghunandan, B. N., and Setoguchi, T., 2004, Simulation of flame spread and turbulent separated flows in solid rockets, AIAA paper, AIAA 2004-3375.